

# Technical Notes

TECHNICAL NOTES are short manuscripts describing new developments or important results of a preliminary nature. These Notes cannot exceed 6 manuscript pages and 3 figures; a page of text may be substituted for a figure and vice versa. After informal review by the editors, they may be published within a few months of the date of receipt. Style requirements are the same as for regular contributions (see inside back cover).

## Effects of Incorporating a Cone Swirler into a Side-Inlet Ducted Ramrocket

Pei-Kuan Wu,\* Ming-Hsiung Chen,\*  
Robert A. Baurle,\* William E. Eakins,†  
and Tzong H. Chen‡  
Taitech, Inc., Beavercreek, Ohio 45440  
and  
Abdollah S. Nejad§  
U.S. Air Force Wright Laboratory,  
Wright–Patterson Air Force Base, Ohio 45433

### Introduction

A RAMROCKET is a dual-mode propulsion system consisting of a solid propellant rocket and an air-breathing ramjet engine.<sup>1</sup> The combustion chamber is initially filled with solid propellant, which is used during the boost flight stage. After the boost stage, the empty chamber is used as a ramjet mode combustor to burn liquid or gaseous fuel during the cruise flight stage. During this stage, side inlets guide ambient air into the combustion chamber and the chemical reaction of air with fuel generates thrust for the missile. The present study was designed to improve the ramjet-mode operation of ramrocket combustors by incorporating a swirler into ramrockets. A generic dual-side-inlet combustor (DSIC) with geometry similar to that of the variable flow ducted rocket combustor<sup>2</sup> was selected as the test problem to demonstrate the advantages of the use of a swirler. The DSIC has two side inlets that are separated at an angle of 90 deg in the azimuthal direction and that intercept the combustion chamber at a 45-deg angle (Fig. 1).

Previous studies of the flow structure and performance of side-inlet ducted combustors in ramjet-mode operations have involved both experimental and computational analyses. Stull et al.<sup>3</sup> studied the flowfields of a dual-inlet side-dump combustor by visualizing air-bubble flows in water-tunnel simulations. Their observations revealed two primary zones: 1) a sometimes bistable recirculating flow in the dome region, and 2) two counter-rotating helical vortices trailing in the streamwise direction from the inlet. Vanka et al.<sup>4</sup> numerically analyzed reacting flowfields in the same ducted rocket configuration. Effects of dome height, side-inlet angle, and injector location were studied, and the utility of computational mod-

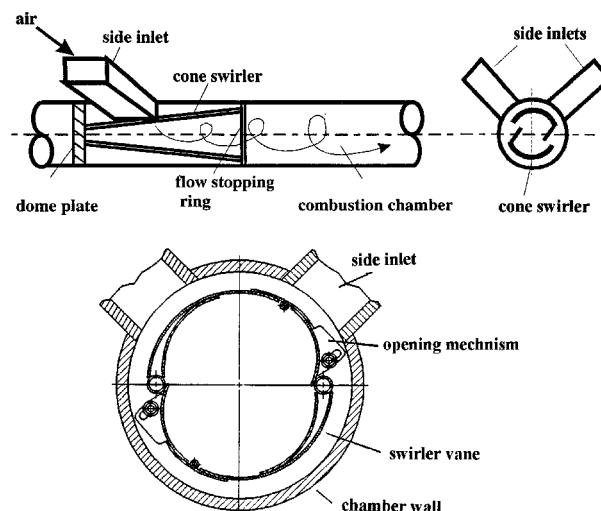


Fig. 1 Installation of a cone swirler in the DSIC combustor.

eling in understanding the ducted rocket combustion process was demonstrated. The recirculation zones observed by Stull et al.<sup>3</sup> can potentially be used as aerodynamic flameholders to stabilize combustion fields. However, the recirculation zone is located too close to the wall and the high reaction temperature, normally over 2000 K, will dramatically heat the wall of the combustion chamber, causing hot spots and sometimes material failure. Furthermore, the high airspeed found in the current DSIC configuration provides very short residence time in the combustion chamber, thus limiting fuel/air mixing and combustion performance.

The objective of this study was to address these issues by evaluating the advantages of installing a swirler in the dome region to generate flow swirl inside the combustion chamber. This approach is an engineering challenge because the swirler has to block the incoming airstream from entering the combustion chamber during the boost stage and release the blockage during ramjet mode operation. A cone swirler was thus designed to meet this requirement and computational simulations were conducted for ducted rockets both with and without the swirler, to demonstrate its advantages. Optimization of the swirler geometry was not attempted and is beyond the scope of this study.

### Design of the Cone Swirler

A cone swirler was designed for installation in the dome region of the combustion chamber (see Fig. 1). The swirler consists of two curved vanes and opening mechanisms. Each vane is divided into two parts: about two-thirds of the total length is fixed in space, while the rest can be hinged inward to produce, when open, an air passage into the combustion chamber. The conical shape of the swirler maximizes the area of the swirler openings and produces vortex breakdown, thus serving as an aerodynamic flameholder. A flow stopping ring is installed at the end of the swirler so that air must pass through the swirler vane opening to enter the combustion chamber. During the boost flight stage, the swirler vanes will be closed, as shown in Fig. 1, to block the incoming airstream.

Presented as Paper 95-2478 at the AIAA/ASME/SAE/ASEE 31st Joint Propulsion Conference and Exhibit, San Diego, CA, July 10–12, 1995; received Aug. 21, 1995; revision received Jan. 11, 1996; accepted for publication July 19, 1996. Copyright © 1996 by the authors. Published by the American Institute of Aeronautics and Astronautics, Inc., with permission.

\*Research Scientist, 3675 Harmeling Drive. Member AIAA.

†Senior Designer, 3675 Harmeling Drive.

‡Chief Scientist, 3675 Harmeling Drive. Senior Member AIAA.

§Senior Research Scientist, Aero Propulsion and Power Directorate.

During ramjet-mode operation, the swirler vanes are opened inward. The swirler unit design is modular and can be rotated to different angles with respect to the side inlets to minimize pressure losses and maximize combustion efficiency. The improvement of combustion efficiency can reduce the length and weight of the combustor, which improves the missile range and agility. In addition, since the swirler redirects airflows, it reduces the sensitivity of the combustor to unequal airstreams from the two side inlets during turning and yawing.

The installation of a swirler into the dome region decreases the available solid propellant storage space, which results in a decrease of the takeover speed at the end of the boost stage. The reduction of solid propellant decreases the total available boost thrust; it also decreases the missile launch weight. On the other hand, the existing air blockage mechanisms can be replaced by the swirler, thus the missile launch weight can be further decreased. Overall, the takeover speed was estimated to decrease by 4%. This loss is not significant as compared to the advantages of the use of a swirler. Nevertheless, the direct contact of the swirler with the high temperature and pressure during the boost stage requires special attention for the selection of swirler materials.

### Computational Methods

Computational simulations of nonreacting flowfields were employed to characterize the flowfields in DSICs with and without swirlers to demonstrate the advantages of using a cone swirler. The KIVA3 program<sup>5</sup> was selected for these simulations because of its ability to handle complex geometries. A detailed description can be found in the KIVA3 program report.<sup>5</sup>

Two grid systems of 60,000 meshes were generated based on the DSIC configuration to simulate flowfields with and without a cone swirler. The grid system of the DSIC without a cone swirler consists of three zones: a combustion chamber and two side inlets. The cylindrical combustion chamber is 60 cm long and has a diameter of 15.2 cm. The two side inlets with a cross-sectional area of  $5.0 \times 8.0 \text{ cm}^2$  intersect the combustor with a dome height of 2.0 cm. For the grid system of the DSIC with a cone swirler, 16 zones were used to generate the approximate shape of the cone swirler. The cone swirler has a conical shape with a diameter increasing from 12.4 to 14.3 cm and a length of 15.0 cm. The vane openings are selected to be 2.2 cm wide in the simulation. A finer grid system with 150,000 meshes for this configuration was also generated and tested to resolve the effects of the law of wall function and the grid dependence. Results are consistent with those from the coarser grid system and do not change the following conclusions.

The boundary conditions for the calculations include inflow, outflow, solid wall, and centerline conditions. The inflow conditions were set by specifying the velocity magnitude and the density at the inlets. These properties were assumed to be uniform across the cross section of the inlet entrances and were selected to be 10,000 cm/s and  $0.00112 \text{ g/cm}^3$ , respectively. The outflow condition was a continuative flow option from the KIVA3 program. The outflow pressure, however, was varied during the calculation to obtain an inlet static temperature of 300 K. This approach allows for the comparison of the two DSIC configurations under the conditions of same mass flow rate, inlet Mach number, and inlet Reynolds number. The boundary conditions on the walls and at the centerline were the law-of-wall and the axis options from the KIVA3 program. The calculations involved more than  $10^4$  cycles and the variations between two consecutive outputs (500 cycles apart) were monitored to assure a converged solution. Root-mean-square velocity values of the variations were maintained under 1 cm/s. Time steps were on the order of  $10^{-4}$  seconds.

### Results and Discussion

The flowfield in a DSIC without a swirler was simulated for comparison with that in a DSIC with a cone swirler. The re-

sults, as seen in Fig. 2, indicate that the incoming airstreams result in four recirculation vortices in the dome area: a pair of stronger vortices located in the lower portion of the combustor and a pair of weaker vortices located in the upper portion of combustor between the two side inlets. These vortices are generated by the strong shear forces between the incoming airstreams and the surrounding air in the chamber. The computed results agree qualitatively with the results of the water-tunnel experiments of Stull et al.<sup>3</sup> The flow patterns gradually reach a fully developed condition near the end of the computational domain, at about four chamber diameters from the dome plate. This result is consistent with the observations of Liou and Wu<sup>6</sup> for a side-inlet dump combustor.

The velocity vector plots for the DSIC with a cone swirler are shown in Fig. 3. The locations of the swirler vanes are darkened in this figure. As shown in the cross-sectional view, the airstreams are redirected by the cone swirler and enter the chamber through the two openings formed by the swirler vanes. Because of the orientation of the swirler openings, the flow structure is not axisymmetric. Nevertheless, most of the flow goes into the swirler directly and produces strong flow swirl in the center of the swirler chamber. Good mixing of fuel and air is expected to take place in this region. The swirl flow in the center portion of the swirler shows vortex breakdown<sup>7</sup> during the expansion process when flow enters the combustion chamber. The vortex breakdown can potentially be used as an aerodynamic flameholder to isolate high reaction temperatures

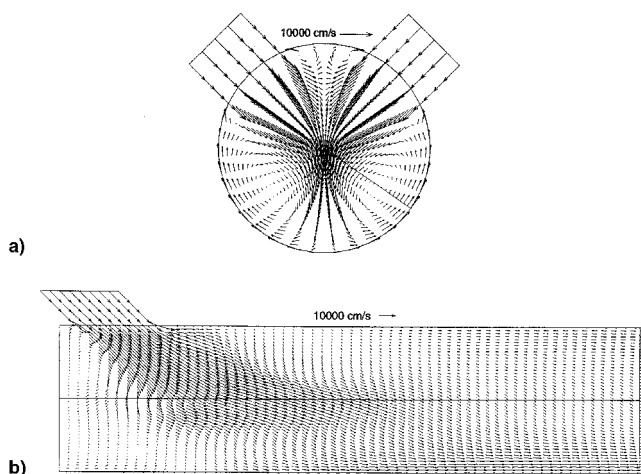


Fig. 2 Velocity vectors for the DSIC without a cone swirler: a) cross-sectional view ( $z = 8$  plane) and b) streamwise view ( $j = 9$  and  $27$  planes).

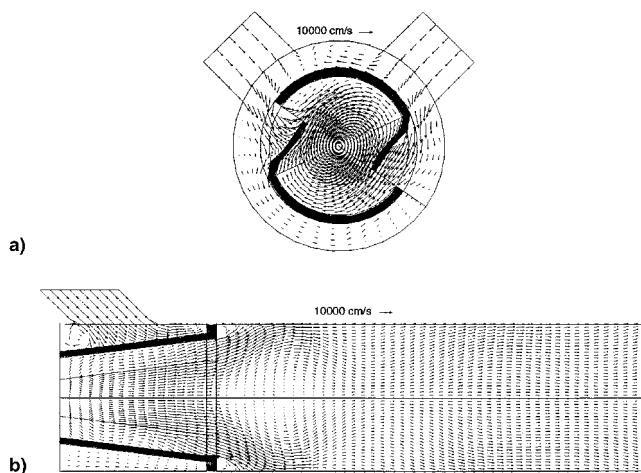


Fig. 3 Velocity vectors for the DSIC with a cone swirler: a) cross-sectional view ( $z = 8$  plane) and b) streamwise view ( $j = 9$  and  $27$  planes).

from the chamber wall and may thus provide better flame stability. No near-wall recirculation zone is generated, thus the hot spot problem can be alleviated.

In the present study, pressure loss is expressed in terms of a stagnation pressure recovery coefficient defined as the ratio of the mass-averaged stagnation pressure at the end of the combustion chamber to the stagnation pressure at the entrance of the side inlets. The recovery coefficient for the original DSIC configuration was found to be 0.96, whereas that of the DSIC with the cone swirler configuration is about 0.79. This pressure loss is acceptable, considering the improvement in fuel/air mixing with improved flow patterns and stronger flow swirl. This pressure loss undoubtedly can be improved as the swirler geometry is optimized.

Flow swirl was quantified as swirl intensity (S.I.), defined as the mass-averaged ratio of tangential kinetic energy to the total kinetic energy. The S.I. is almost zero for the original DSIC design, except near the dome region, because mixing in the DSIC is only significant in the shear layers between the incoming airstreams and the surrounding air. For the DSIC with a cone swirler the S.I. is larger than 0.3 throughout the combustion chamber, which is a significant improvement on the original DSIC configuration.

### Summary

A feasible cone swirler design for a side-inlet ducted ram-rocket combustor has been demonstrated and its advantages illustrated using the KIVA3 program. Studies of the nonreacting flowfield indicate that the cone swirler not only improves the flow pattern, but also enhances the flow swirl in the combustor. Use of the cone swirler should result in better fuel/air mixing and more complete combustion in the combustion chamber, without significant pressure losses. The primary recirculation zone is generated by vortex breakdown and is located at the combustor center; it can be used as an aerodynamic flameholder to stabilize the reacting field. It is thus anticipated that the DSIC with a cone swirler will be more efficient than the DSIC without a swirler. The swirler concept is general and can be applied to combustors with different geometries. To quantify the effects of pressure losses on missile thrust, however, reacting flows must be studied.

### Acknowledgments

This study was supported by and performed at Wright-Patterson Air Force Base, under Contract F33615-94-C-2439. Additional support was a grant of CRAY computer time from the Department of Defense CEWES High Performance Computing Center. The authors would like to thank A. A. Amsden of the Los Alamos National Laboratory for many valuable comments about the KIVA3 program, and A. E. S. Creese of Taitech, Inc., for editorial comments concerning this article.

### References

- <sup>1</sup>Timnat, Y. M., "Recent Developments in Ramjets, Ducted Rockets and Scramjets," *Progress in Aerospace Science*, Vol. 27, No. 3, 1990, pp. 201-235.
- <sup>2</sup>Slagle, D. R., and Braendlein, R. K., "Variable Flow Ducted Rocket (VFDR) Program," Air Force Wright Aeronautical Labs., TR-82-2130, Wright-Patterson AFB, OH, Jan. 1983.
- <sup>3</sup>Stull, F. D., Craig, R. R., Streby, G. D., and Vanka, S. P., "Investigation of a Dual Inlet Side Dump Combustor Using Liquid Fuel Injection," *Journal of Propulsion and Power*, Vol. 1, No. 1, 1985, pp. 83-88.
- <sup>4</sup>Vanka, S. P., Craig, R. R., and Stull, F. D., "Mixing, Chemical Reaction, and Flowfield Development in Ducted Rockets," *Journal of Propulsion and Power*, Vol. 2, No. 4, 1986, pp. 331-338.
- <sup>5</sup>Amsden, A. A., "KIVA-3: A KIVA Program with Block-Structured Mesh for Complex Geometries," Los Alamos National Lab., Rept. LA-12503-MS, March 1993.
- <sup>6</sup>Liou, T.-M., and Wu, S.-M., "Flowfield in a Dual-Inlet Side-Dump Combustor," *Journal of Propulsion and Power*, Vol. 4, No. 1, 1988, pp. 53-60.

<sup>7</sup>Escudier, M. P., and Keller, J. J., "Recirculation in Swirling Flow: A Manifestation of Vortex Breakdown," *AIAA Journal*, Vol. 23, No. 1, 1985, pp. 111-116.

## Payload to Low Earth Orbit by Aerospace Plane with Scramjet Engine

Takeshi Kanda\* and Kenji Kudo†  
National Aerospace Laboratory,  
Kimigaya, Kukuda, Miyasi 981-15, Japan

### Introduction

Aerospace plane is being studied as the new transportation system to low earth orbit (LEO). The propulsion system of the aerospace plane requires several engines: an air-turbo-ramjet engine (ATR), a scramjet engine, and a rocket engine.

In the present research, the characteristics and role of the scramjet for the single-stage aerospace plane were investigated for a LEO of 100 km. The scramjet engine is usually fueled by hydrogen, although there are several studies on the hydrocarbon-fueled scramjet engines.<sup>1,2</sup> Therefore, the possibility of using methane as well as hydrogen was investigated, and the size of the payload that could be carried by various combinations of the engines was estimated.

### Calculation Procedure

#### Flight Simulation

The aerospace plane was treated as a material point. The motion of the aerospace plane was within the horizontal and vertical plane. The schematic diagram of the forces is shown in Fig. 1, and the equations used in the study are given as follows:

$$\frac{dx}{dt} = \frac{R}{R+z} \cdot v \cdot \cos \gamma \quad (1)$$

$$\frac{dz}{dt} = v \cdot \sin \gamma \quad (2)$$

$$\frac{dv}{dt} = \frac{F \cdot \cos \delta - D}{m} - g \sin \gamma \quad (3)$$

$$\frac{d\gamma}{dt} = \frac{F \cdot \sin \delta + L}{m \cdot v} - \frac{g \cdot \cos \gamma}{v} + \frac{v \cdot \cos \gamma}{R+z} \quad (4)$$

$$\frac{dm}{dt} = -\frac{F}{I_{sp}} \quad (5)$$

In the equations,  $x$ ,  $t$ ,  $R$ ,  $z$ ,  $v$ , and  $\gamma$  are distance on the Earth surface, time, the radius of the Earth, height, velocity, and angle of inclination, respectively.  $F$ ,  $\delta$ ,  $D$ ,  $m$ , and  $g$  are force, angle between the engine thrust and the airframe velocity,

Received July 31, 1995; revision received July 18, 1996; accepted for publication Aug. 2, 1996. Copyright © 1996 by the American Institute of Aeronautics and Astronautics, Inc. All rights reserved.

\*Senior Researcher, Ramjet Propulsion Research Division, Kakuda Research Center. Member AIAA.

†Senior Researcher, Ramjet Propulsion Research Division, Kakuda Research Center.